J10.2

SOIL MOISTURE EFFECTS ON GASEOUS EXCHANGES BETWEEN THE ATMOSPHERE AND THE BIOSPHERE

Yihua Wu[1], Christa Peters-Lidard[1], Robin Dennis[2], and Peter Finklestein[2].

ABSTRACT

The multi-layer biochemical dry deposition model (MLBC) was coupled with the community NOAH land-surface model (LSM) to investigate effects of soil type and soil moisture on gaseous exchanges between the atmosphere and the biosphere. The MLBC is a resistance model, an analog to Ohm's law. Some detailed bio-chemical processes that affect dry deposition are considered in the model. Parameterizations of aerodynamic, boundary layer, stomatal, cuticular and soil surface resistances are updated with new findings in recent research. The model is designed for use in nationwide dry deposition networks, e.g. the Clean Air Status and Trends Network (CASTNet); and in mesoscale air quality models. The NOAH LSM model computes the surface energy and water balances, and produces realistic soil moisture conditions. Almost, every resistance terms in the MLBC model, such as, aerodynamic resistance, stomatal resistance and soil surface resistance are strongly linked with available soil water content. Soil moisture saturation point, field capacity and wilting point vary with soil types, and so does the available soil water content. In this study, we conducted two numerical experiments: modeling CO_2, O_3, SO_2 and H_2O (latent heat) fluxes under wet, dry and optimal soil moisture conditions, and modeling these fluxes with the same soil moisture content for 8 soil types. The preliminary results show that soil moisture effect on the modeled fluxes is significant.

1. HSB, NASA/GSFC, Greenbelt, MD 20771
2. ASMD, US EPA, Research Triangle Park, NC 27711

1. INTRODUCTION

Land-atmosphere gaseous exchanges have detrimental impacts on atmospheric chemistry, ecosystem health and climate changes. Field measurement methods and numerical models have been developed to quantify these exchanges and assess their effects (Bennett et. al., 1973; Wesely, 1989; Hicks et. al, 1991; Katul et. al., 1996; Meyers et. al., 1998; Pleim et. al., 1999; Finkelstein et al, 2000; Wu et al, 2002). A common simulation method used to calculate gas exchange is an analog to Ohm's law, the resistance model of gas transfer, and can be expressed as:

$$F_c = \frac{C_a - C_i}{R_{Total}} \tag{1}$$

where F is the flux of a specific gas; C_a and C_i are the ambient and surface (or intercellular) gas concentrations, respectively; R_{Total} is the total resistance that usually includes the aerodynamic resistance for the turbulent layer (R_A), the laminar layer resistance for the quasi-laminar layer (R_B) and the surface or canopy resistance for the receptor itself, in series. The canopy resistance includes the stomatal and cuticular resistance (R_S and R_{Cut}) as well as the soil surface resistance (R_{Soil}) in parallel.

Almost, every resistance term, especially, stomatal resistance and soil surface resistance are strongly linked with available soil water content. Soil moisture saturation point, field capacity and wilting point vary with soil types, and so does the available soil water content. Therefore, it is expected that soil moisture conditions and soil types have effects on the land-atmosphere gaseous exchanges. To investigate these effects, the multi-layer biochemical dry deposition model (MLBC) developed by Wu et al (2002) was coupled with the community NOAH land-surface model (LSM) described by Chen et al (1997), and was run with measurements taken from a soybean field at Nashville, TN in 1997. Readers are referred to Meyers et al. (1998) for detailed description about the site and measure method. Two numerical experiments were conducted: modeling CO_2, O_3, SO_2 and H_2O (latent heat) fluxes under wet, dry and optimal soil moisture conditions, and modeling these fluxes with the same soil moisture condition for 8 soil types. Both measured and modeled fluxes are half hourly. Data used in this study are selected based on the data quality control by Meyers et al. (1998). Results from the two experiments are analyzed in Section 2 and 3. A short summary is presented in Section 4.

2. EXPERIMENT ONE—SOIL MOISTURE EFFECT

In this experiment, the coupled model was run for three soil moisture cases: Dry, Wet and Opt. The initial soil moisture for the three cases is given in Table 1. The single-diagram method described by Taylor (2001) was used for comparisons. This method provides a concise statistical summary of how well model outputs match measurements in terms of their correlation, their standard deviations, and centered pattern root-mean-square difference. In this diagram, the correlation coefficient (*R*) is shown as the radial angle, the standard deviations (σ_m for model and σ_o for observations) as the radial distance. The observations are plotted on the horizontal axis since they are perfectly correlated with themselves (*R*=1). The centered pattern root-mean-square difference (E') is the vector distance between the observation (on the horizontal axis) and the corresponding modeled point. The relationship between E' and *R*, σ_m and σ_o can be expressed as $E' = \sqrt{\sigma_o^2 + \sigma_m^2 - 2\sigma_o \sigma_m R}$. The larger the correlation coefficient, the better the match between the modeled and observed phases of seasonal and diurnal cycles; the closer the standard deviation of the model to the observation, the better the estimation of the amplitude of variations (seasonal and diurnal cycles); the smaller the centered pattern root-mean-square difference, the closer correspondence between the model and the observations.

Table 1. Initial soil moisture condition in the Dry, Wet and Opt cases

Layer	Depth (m)	Total soil moisture			Liquid soil moisture		
		Dry	Wet	Opt	Dry	Wet	Opt
1	0.1	0.2252	0.4252	0.3252	0.1260	0.3260	0.1660
2	0.3	0.2195	0.4195	0.3195	0.1828	0.3828	0.2828
3	0.6	0.2172	0.4172	0.3172	0.2172	0.4172	0.3172
4	1.0	0.2078	0.4078	0.3078	0.2078	0.4078	0.3078

The values of σ_m, σ_o, R and E' for measured and modeled fluxes in the three cases are shown in Figure 1(a) (CO_2), 1(b) (H_2O), 1(c) (O_3) and 1(d) (SO_2). The correlation coefficients between the measured and simulated fluxes for the each gas species are almost identical in the Dry, Wet and Opt cases. These indicate that the model-simulated seasonal and diurnal cycles of each gas species are almost the same in-phase for the three cases. However, the standard deviations (σ_m) in the three cases are different: the smallest for the Dry case. Comparisons of standard deviations between model-simulated and observed data show that the model overestimated the amplitudes of seasonal and diurnal variations of CO_2 flux in the Opt case, but underestimated in the Dry and Wet cases. The model underestimated the amplitude of H_2O and O_3 flux, but overestimated the amplitude of SO_2 flux in all cases. The E' value is the largest in the Dry case. The figure shows that the contribution of σ_m to E' is larger than contribution of R in the three cases. The figures suggest that soil moisture stress due to water-logging and drought can cause the closure of stomata, but the degree of stomata closing is higher in drought conditions than in water-logging conditions. Among the four gas species, CO_2, H_2O and O_3 have higher correlation coefficients than SO_2 does, suggesting that SO_2 might have some different exchange pathways from the other three.

The weekly daytime (Local time 09:00—15:00) averages and average hourly values of modeled CO_2, O_3, SO_2 and H_2O fluxes, and the corresponding measurements were analyzed to show soil moisture effect on the amplitudes of modeled seasonal and diurnal cycles of atmosphere-biosphere gas exchanges (data not shown). Results indicate that soil moisture effect is larger during summer and noon time.

3. EXPERIMENT TWO—SOIL TYPE EFFECT

The coupled model was run for 8 soil types (Table 2) in this experiment. Taylor's single diagram was also used for analysis. The values of σ_m, σ_o, R and E' for fluxes of CO_2, H_2O, O_3 and SO2 for the 8 soil types are shown in Figure 2(a), 2(b), 2(c) and 2(d), respectively. There are no big differences in the correlation coefficients among the 8 simulations for each gas species. These indicate that the timings of the model-simulated seasonal and diurnal cycles of each gas species are almost the same for all of the soil types. However, the differences in the standard deviations among the 8 run are clear.

The standard deviation has the largest value in the run with soil type 1 and the smallest value in the run with soil type 3 for all of the gas species. Comparisons of standard deviations between model-simulated and observed data show that the model overestimated the amplitudes of seasonal and diurnal variations of CO_2 flux in the runs with soil type 1, 4, 5, 7 and 8, but underestimated in the runs with soil type 2, 3 and 6. The model underestimated the amplitudes of seasonal and diurnal variations of H2O and O3 fluxes in all runs, but overestimated the amplitudes of seasonal and diurnal variations of SO2 fluxes in all runs. Comparison between the order of the standard deviations (from the smallest to the largest) in Figure 2 with the order of wilting points in Table 2 shows that the wilting point is the critical parameter that has the most impact.

The weekly daytime (Local time 09:00—15:00) averages and average hourly values of modeled CO_2, O_3, SO_2 and H_2O fluxes (data not shown) for the 8 runs show that soil type effect on the amplitudes of modeled seasonal and diurnal cycles of atmosphere-biosphere gas exchanges is larger during summer and noon time.

Table 2. Soil types and the corresponding parameters

Number	Name	Wilting Point	Saturation Point	Reference Point
1	Loam Sand	0.029	0.421	0.283
2	Silty Clay Loam	0.119	0.464	0.387
3	Light Clay	0.139	0.468	0.412
4	Sandy Loam	0.047	0.434	0.312
5	Sandy Clay	0.100	0.406	0.338
6	Clay Loam	0.103	0.465	0.382
7	Sandy Clay Loam	0.069	0.404	0.315
8	Loam	0.066	0.439	0.329

4. SUMMARY

The multi-layer biochemical dry deposition model (MLBC) was coupled with the community NOAH land-surface model (LSM) to investigate effects of soil type and soil moisture on gaseous exchanges between the atmosphere and the biosphere. Two numerical experiments were conducted. In experiment one, CO_2, O_3, SO_2 and H_2O (latent heat) fluxes were simulated under wet, dry and optimal soil moisture conditions. In experiment two, these fluxes were simulated with the same soil moisture content for 8 soil types. Analysis shows that soil moisture and soil types have the mostly impact on the amplitudes of seasonal and diurnal variations of the exchange flux of each gas species, but little effect on phases of the model-simulated seasonal and diurnal cycles of the exchange flux of each gas species. The effects of soil moisture and soil types on the amplitudes of the model-simulated seasonal and diurnal cycles are larger during summer and noon time.

REFERENCE

Bennett, J.H., A.C. Hill and D.M. Dates, A model for gaseous pollutant sorption by leaves. *J. Air Poll. Control Assoc.*, **23**, 957-962, 1973.

Chen, F., Z. Janjic, and K. Mitchell, Boundary-Layer Meteorol, 85, 391-421, 1997

Finkelstein, P.L., T.G. Ellestad, J.F. Clarke, T.P. Meyers, D.B. Schwede, E.O. Hebert, and J.A. Neal, Ozone and sulfur dioxide dry deposition to forests: observations and model evaluation. *J. Geophys. Res.*, **105**, 15365-15377, 2000.

Hicks, B.B, R.P. Hosker, T.P. Myeres and J.D. Womack, Dry deposition measurement techniques I. Design and tests of a prototype meteorological and chemical system for determining dry deposition. *Atmos. Environ.*, **25**, 2345-2359, 1991.

Katul, G.G., P.L. Finkelstein, J.F. Clarke and T.G. Ellestad, An investigation of the conditional sampling method used to estimate fluxes of active, reactive, and passive scalars, *J. Applied Meteorol..*, **35**: 1835-1845, 1996.

Meyers, T.P., P.L. Finkelstein, J. Clarke, T.G. Ellestad and P. Sims, A multilayer model for inferring dry deposition using standard meteorological measurements. *J. Geophys. Res.*, **103**, 22645-22661, 1998.

Pleim, J. E., P.L. Finkelstein, J.F. Clarke and T.G. Ellestad, A technique for estimating dry deposition velocities based on similarity with latent heat flux. Atmospheric Environment, **33**: 2257-2268, 1999.

Taylor, K. E., Summarizing multiple aspects of model performance in a single diagram. *J. Geophys. Res*., **106**, 7183-7192, 2001.

Wesely, M.L, Parameterization of surface resistance to gaseous dry deposition in regional-scale numerical models. *Atmospheric Environment*, **23**, 1293-1304, 1989.

Wu, Y., B. Brashers, P. L. Finkelstein and J. E. Pleim, A Multi-layer bio-chemical dry deposition model, Part I: Model Formulation, *J. Geophys Res*., Accepted, 2002.

Wu, Y., B. Brashers, P. L. Finkelstein and J. E. Pleim, A Multi-layer bio-chemical dry deposition model, Part II: Model Evaluation, *J. Geophys Res*., Accepted, 2002.

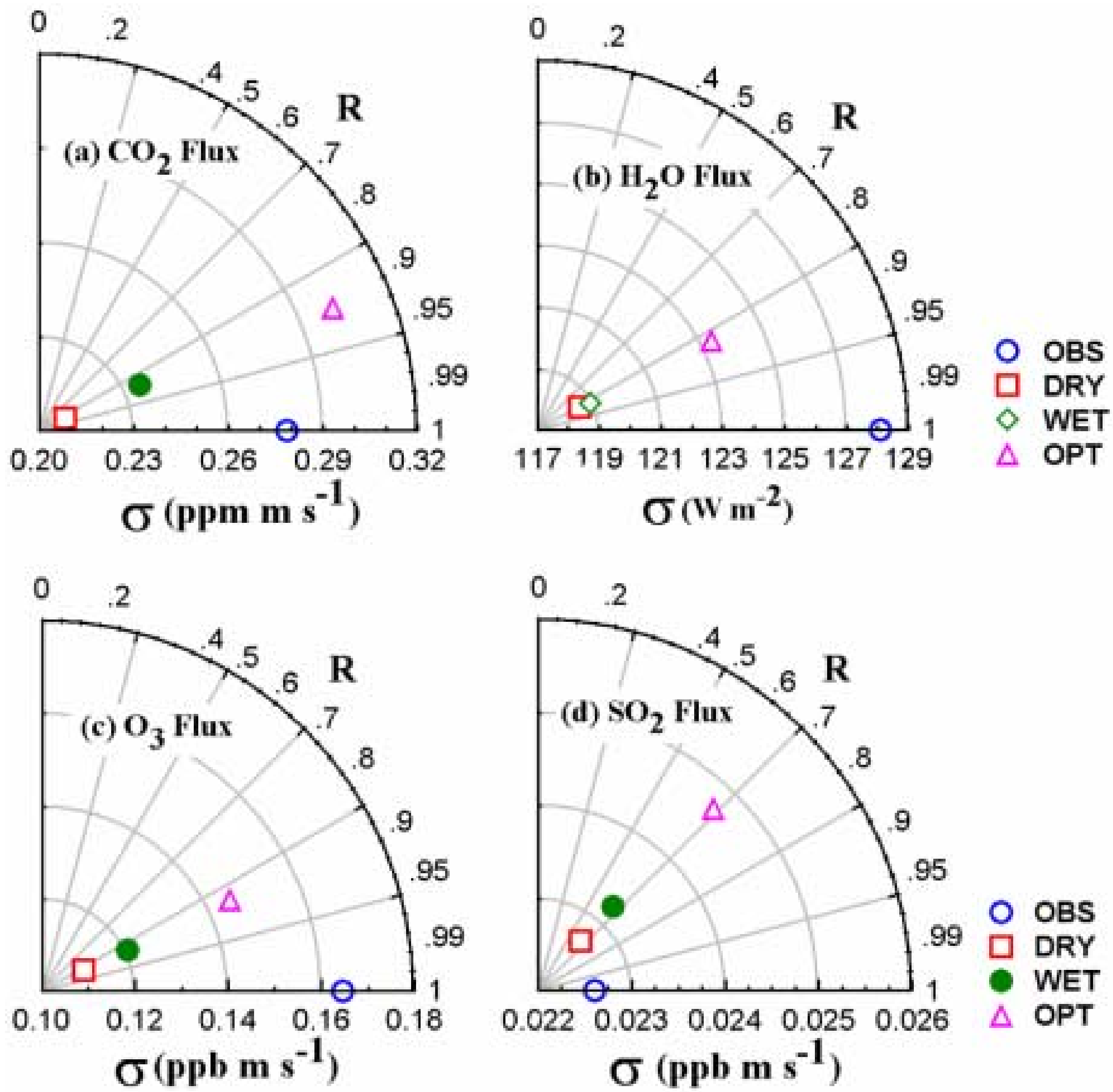

Figure 1. Comparisons between modeled and observed fluxes in the three runs. The correlation coefficient (*R*) is shown as the radial angle, the standard deviations (σ) as the radial distance, and the centered pattern root-mean-square difference (E') as the vector distance between the observation (on the horizontal axis) and the corresponding modeled point, for (a) CO_2 flux, (b) H_2O flux, (c) O_3 flux, and (d) SO_2 flux.

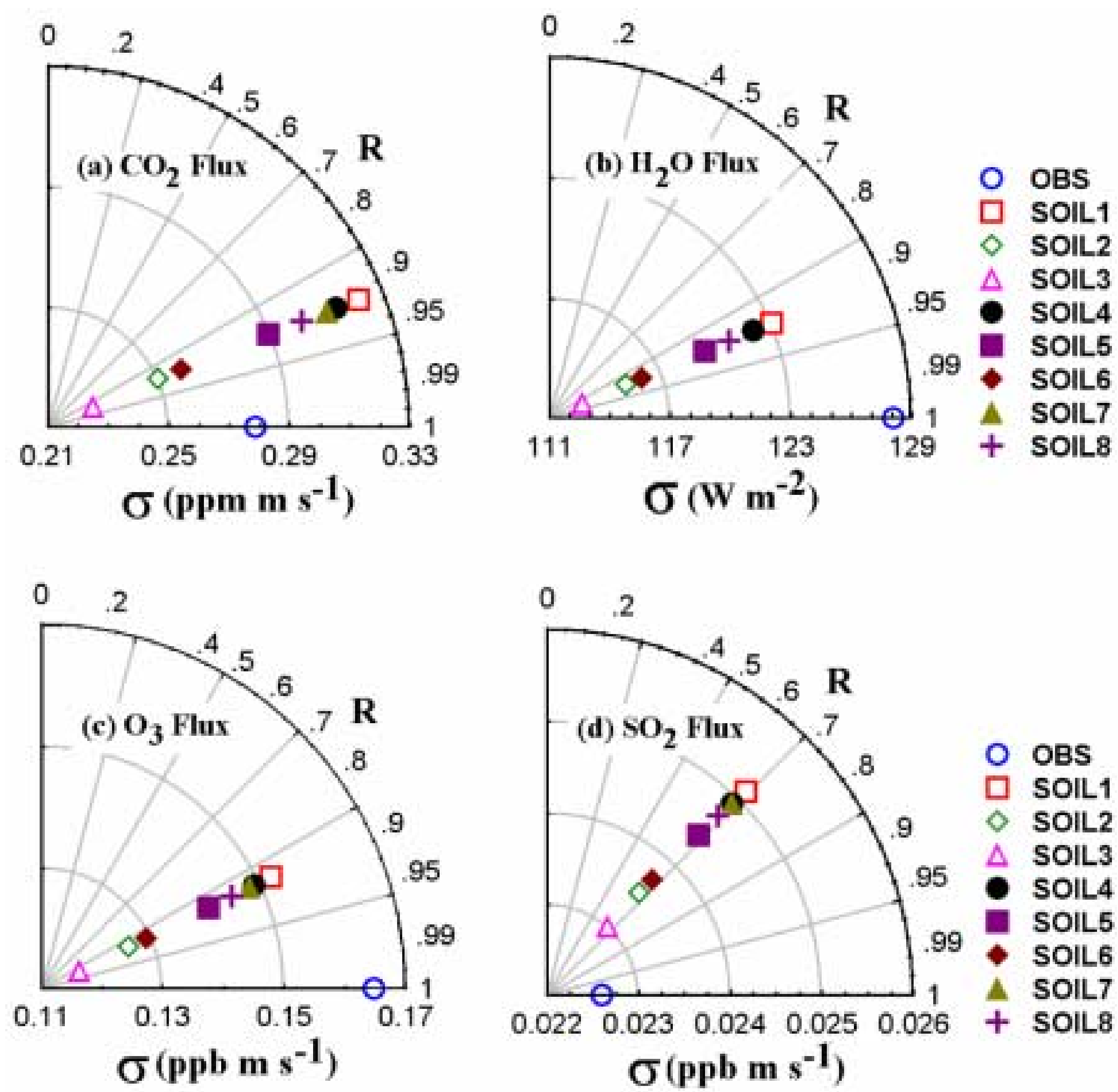

Figure 2. Comparisons between modeled and observed fluxes in the 8 runs with 8 soil types. The correlation coefficient (*R*) is shown as the radial angle, the standard deviations (σ) as the radial distance, and the centered pattern root-mean-square difference (E') as the vector distance between the observation (on the horizontal axis) and the corresponding modeled point, for (a) CO_2 flux, (b) H_2O flux, (c) O_3 flux, and (d) SO_2 flux.